Mechanism for retarding the nucleation rate in a dense nonneutral ion plasma

S. V. Shevkunov

St. Petersburg State Technical University

Results of computer modeling of a symmetric 1-1-valent ionic plasma reveal that ion microclusters display an anomalously rapid switch in their thermodynamic behavior to the extensive properties characteristic of a macroscopic system. This effect is explained by the strong shielding of the electrostatic interaction of the ions in the liquid phase and has significant consequences for the nucleation mechanism in a dense symmetric plasma. In a plasma in which the charged symmetry of the ions is violated the nucleation mechanism changes qualitatively. Near the gas–liquid coexistence curve the plasma is organized into a gas of ion triplets, and the orientation forces between the triplets interfere with the formation of dense-phase nuclei. In order to investigate the mechanism for the retardation of nucleation, the lattice approximation and the physical-group approximation have been introduced and the Monte Carlo technique has been used to simulate the process in an isothermal and isobaric statistical ensemble.

The conventional approach in the theoretical description of atomic and molecular systems by means of statistical mechanics is to expand in power series in a small parameter. Examples of this approach are the virial expansion in equilibrium statistical mechanics,[1–15] linear perturbation theory in nonequilibrium statistical mechanics,[16–18] and perturbation techniques in quantum mechanics.[19–21] But a small parameter is by no means always available to theory. Approximate theories of this type are asymptotically correct as the small parameter approaches zero; the most interesting regions, e.g., the region of phase transitions in highly nonideal systems, are not accessible to them.

In the middle of the 1950s a fundamentally new approach in the description of molecular systems became possible: numerical modeling with computers.[22–38] One area for the application of such mathematical modeling techniques is that of small systems of particles. Numerical modeling methods in this area have a special role because of the absence of rigorous analytical approaches to the statistical description of systems whose dimensions are comparable with those of their constituent particles.

Success in an analytical approach to the statistical-mechanical description of a very nonuniform atomic or molecular system depends on a number of simplifying circumstances. These include, among others, a small interparticle correlation length in comparison with the typical dimensions of the microscopic irregularities. The use of local thermodynamic properties, such as the surface stress at the phase boundary, the chemical potentials of the phase, and the local pressure, presupposes that local regions inside the nonuniform system are sufficiently isolated from one another. This isolation is necessary because the apparatus of the Gibbs statistical ensembles, and hence the possibility of going from a microscopic description to a simplified thermodynamic description, requires that the weak interaction between the system and the reservoir vanish in comparison with the interactions within the system.[39] The Gibbs distribution remains valid even in the absence of a thermodynamic limit as the particle number increases, $N \to \infty$. A small system continues to obey the Gibbs distribution regardless of its size, provided that the interaction with its environment is vanishingly weak.[39] This does not mean that the small system size does not introduce a number of features into the application of the method of statistical ensembles. The absence of a thermodynamic limit requires that the relative fluctuations be finite: the average differs from the most probable value, which makes the description in different statistical ensembles inequivalent.[40,41] However, this inequivalence is not a defect of the theory; it reflects the physical inequivalence of different ways of distinguishing a small system from its macroscopic environment.

There are a number of reasons for the interest in studying small systems. On the one hand, the properties of individual atomic clusters, molecules, or ions can have a crucial effect on the behavior of macrosystems. The clearest example of this is afforded by the condensation process, whose rate is determined by the thermodynamic properties of the critical seeds.[42] In the Frenkel–Band theory[43–46] a nonideal gas is described as a mixture of clusters of different sizes: dimers, trimers, etc. A particle cluster in a gas can be regarded as an isolated object, since the time needed to establish equilibrium within the cluster is considerable less than the interval between collisions of the cluster with gas particles. On the other hand, small systems of this sort are interesting from the standpoint of statistical theory. There is general interest in the answers to the questions, at what number of particles do collective effects appear and to what extent do they give rise to phase transitions in macrosystems.

There is particular interest in clusters of charged particles. As is well known, attempts to develop a theoretical description for systems of charged particles in the very nonideal region are complicated by the long-range nature of the Coulomb interaction. Even when the density de-

creases, collectivization in the system does not cease as is the case with short-range forces; on the contrary, it increases by virtue of the rapid increase in the size of a Debye sphere.[47–51] Shielding turns out to be the only factor that prevents the thermodynamic potentials from diverging, and must be taken into account even in evaluating group integrals. The idea of expanding group integrals in clusters with simpler connections and then regrouping them was suggested by Mayer.[3,5,8,11] In principle this permits one to write down expressions for the virial coefficients in terms of convergent cluster integrals. Application of the convolution theorem in the summation of the Fourier transforms of ring diagrams leads to the Debye potential of the average force between the ions. The contributions from the other diagrams reduce to "prototype diagrams" with Debye screening in the connections responsible for their convergence, and they can be regarded as corrections of higher order in the density to the Debye limit of the law. Despite its elegance, the Mayer theory is still an asymptotic theory for low densities and high temperatures. The question of the radius and rate of convergence of these expansions remains open, and the expansions themselves can only aspire to the role of small corrections to the Debye limit, and are not in a position to describe the qualitative structural changes and the related nonmonotonic behavior of the thermodynamic properties of an ion plasma at intermediate densities and temperatures. Consequently, the most important specific results for ion systems have been obtained not from virial expansions but by methods usually employed in the theory of liquids, namely integral-equation methods.[52–60]

The cluster approach to the problem of describing the thermophysical properties of very nonideal gases reduces to identifying the leading contributions to the statistical integral by dividing the phase space of the system into regions. Each region is associated with some subdivision of the macrodivision into clusters. The location of the boundaries between regions depends on the specific definition of the physical cluster and allows a well-known arbitrariness, since the result of the calculations varies slightly as the locations of the boundary change if the latter pass through phase points corresponding to improbable molecular configurations. If the problem consists of just calculating equilibrium properties, the statistical integral reduces after a trivial integration over momenta to an integral in terms of the molecular coordinates only, i.e., a configuration integral. In this case the cluster subdivision of phase space reduces to a subdivision of configuration space; including the kinetic properties in the definition of a cluster does not make the theory more accurate. Then an accurate general cluster theory can be developed regardless of the specific definition of the cluster.[41]

In the kinetic theory of nucleation the steady rate of cluster formation is expressed in terms of the equilibrium properties of the nucleate. Thus, the calculation of the equilibrium properties of clusters (the nucleate) of a dense gas is the central problem of the theory of homogeneous nucleation. The exponential dependence of the rate of formation of the nucleate on its free energy imposes severe requirements on the accuracy with which the latter is evaluated.

PRINCIPAL RESULTS OF NUMERICAL MODELING, KNOWN FOR THE INTERNAL PHASES OF A NONIDEAL ION SYSTEM

Systematic studies of the equilibrium properties of 1–1-valent charged spheres using the Monte Carlo method began with the calculation of the high-temperature isotherm corresponding to an aqueous solution of a 1–1-valent electrolyte at room temperature in the canonical NVT statistical ensemble.[61,62] A nearby isotherm was studied by the Monte Carlo method in Ref. 63. The results for the osmotic coefficients from Ref. 62 were compared with the hyperchain approximation in Ref. 64. The results of the Monte Carlo calculation for $T = 298$ K and $N = 32$, 64, and 200 ions in periodic geometry were compared systematically with the numerical solution of the Percus–Yevick integral equation, the spherical model, and the hyperchain approximation in Ref. 65. This showed that the hyperchain approximation yields answers that are closest to those obtained with the Monte Carlo method. Liquid-state calculations of an ion system with a Huggins–Mayer and Poling ion-ion potential were carried out in Refs. 66–72. Valleau and Card[73] developed a method for calculating the density of States by the Monte Carlo method and a way of overcoming normalization difficulties. Chasovskikh and Vorontsov–Vel'yaminov used the Monte Carlo method to calculate the same isotherm as in Ref. 65, but with an isothermal-isobaric NpT ensemble. The rules governing the sharp increase in two-particle correlations (the formation of ion pairs) were established. A deviation in the behavior of the binary distribution functions from the Debye distribution was observed in the pairing region only at distances close to contact. Kinks were observed here in the temperature dependence of the thermal coefficients. These structural alterations in the system were interpreted[74] as a transition from many-particle shielding of the opposite ion in the Debye region to shielding by a single opposite ion. It is well known that for charged-particle systems strong long-range correlations in the particle positions exist both at high density ("liquid" oscillations of the binary distribution function) and at low ("gaslike") density. The latter are associated with the fact that the correlation distance in a low-density system is the Debye radius, which increases as the density decreases and the temperature rises. Consequently, for higher densities in the system of charged particles a point must be observed at which the correlation length is a minimum. The region of minimum correlations has been studied along two isobars.[75] As the temperature drops the correlation length decreases to its minimum value, at which time the binary distribution function undergoes a qualitative change: weak antiphase oscillations develop, which grow in amplitude as the temperature subsequently decreases, and spread out over large distances. The thermal coefficients calculated from the fluctuation formulas have finite discontinuities at the point where the minimum correlations occur. At approximately the same parameter range, corresponding to the condition of screen-

ing by a single opposite ion, independent Monte Carlo calculations of the 1-1-valent charged-sphere model were carried out by Zelener et al.[76] They studied the deviations of the energy and pressure from the limiting values of the Debye laws as the departure from ideal behavior increased.

Calculations of one isotherm and one isobar in the supercritical region in the NpT ensemble of a system of ions with weak repulsion ($\propto r^{-8}$) was carried out in Ref. 77. Introducing a soft short-range force in the ion-ion potential does not affect the presence of a boundary in the phase diagram between the Debye region and the ion-pairing region. An asymmetric NaCl+KCl mixture with a Huggins–Mayer potential in the liquid-state region was simulated by Larsen et al.[78] Reference 79 discussed the similarity relation for the internal energy in the charged-sphere model.

The first gas-phase approach to the dense phase in a charge-symmetric 1-1-valent ion macrosystem was studied in Ref. 80 in an NpT statistical ensemble using the nearest-image technique.[61] In Refs. 81–84 the same technique was used to estimate the critical parameters of the system. Comparison of the data from Ref. 84 for the energy with the calculations of Larsen[85] at low temperatures in the high-density region reveal that the results of Ref. 84 are lower by 10–15% than the corresponding values from Ref. 85. On the other hand, for the gaseous branch the results of Refs. 84 and 85 are in good agreement. In Ref. 85 the Ewald procedure was used to treat the long-range interactions, while in the calculations of Ref. 84 the nearest-image technique was used. In Refs. 86 and 87 the equations of state along three isotherms for the 1-1-valent charged-sphere model and three isotherms for the model with a "soft" short-range part $\propto r^{-8}$ were calculated to determine the phase transition in the system with long-range interactions. Using the Ewald method to include long-range interactions reduces the critical pressure by more than a factor of ten, the critical temperature by 20–30%, and the critical density severalfold. Comparison of the results of the numerical simulation with indirect data from a laboratory experiment[88] for K^+Cl^- and Na^+Cl^- reveals that the agreement is quite satisfactory for the critical parameters of the 1-1-valent charged-sphere model.

For the points of the gaseous branch the contact value of the binary distribution function $g_{+-}(r)$ for oppositely charged ions is typically extremely large and the binary distribution functions $g_{++}(r)$ and $g_{--}(r)$ for like-charged ions have a strong maximum at distances of two particle diameters. Sequences of configurations exhibit separate pairs of oppositely charged ions and, less often, clusters of three ions. For the liquid branch the contact value of $g_{+-}(r)$ is smaller by more than a factor of ten; for both binary distribution functions antiphase oscillations are typically observed. Sequences of configurations in the dense phase consist of a network of long convex branching chains with a succession of ions having opposite signs. Note the anomalously large value of the critical volume of the ion system. Thus, for water the critical volume is three times the dense-packing volume and the factor is the same for

argon; for the 1-1-valent charged-sphere model it is a factor of ten.

Based on the data from numerical modeling, a number of regions can be distinguished in the VT diagram. At high temperatures the region of weak correlations (the Debye region) for small specific volumes goes directly into the region where the structure is close to a dense system of hard spheres with in-phase oscillations of both types of binary distribution function. At lower temperatures the Debye region abuts the ion-pairing region, in which these functions are monotonic but differ considerably from the Debye distributions at short distances. The curve constituting the boundary between these regions is characterized by anomalies in the behavior of the specific heats and other equilibrium properties, and its location in the phase diagram approximately corresponds to where the Debye and Björrum radii coincide. Another boundary in the diagram separates the region where the binary distribution functions vary monotonically (the ion-pairing region) from the oscillatory distribution (the three-body correlation region), and corresponds to the minimum in the correlation length. The gas–liquid coexistence curve corresponds to temperatures that are several times lower than the first two boundaries for the same values of the volume. The presence of these boundaries confirms the results of the calculation by an independent method using the theory of physical groups.[89,90]

In Refs. 91 and 92 the Monte Carlo method was used with an NpT ensemble to study the thermodynamic properties of an asymmetric two-component macrosystem of charged spheres with ion charges $+2$ and -1 (model 2) along the three isotherms $T_1=0.287$, $T_2=0.125$, and $T_3=0.072$.[1] The configuration energy in a unit cell with 48 particles was evaluated using the Ewald method, i.e., partial summation in the reciprocal space. The study of the asymmetrical system by the Monte Carlo method was continued in Ref. 93. The low-temperature isotherm T_3 has a discontinuity corresponding to the gas–liquid phase transition. Estimates of the critical parameters for the system in question ($p_c=10^{-3}$, $v_c=10$, $T_c=0.1$) in comparison with the critical parameters of model 1 ($p_c=10^{-3}$, $v_c=10$, $T_c=0.06$) reveal that the phase transition in model 2 occurs at higher temperature. In the behavior of the compressibility factor $\Phi=pv/T$ the Coulomb attractive forces ($\Phi<1$) dominate in the region of molar densities $10^{-1}>\rho>10^{-6}$; for $\rho>10^{-1}$ the system displays typical liquid behavior. The Boyle point $\Phi=1$ corresponds to the value $v=\rho^{-1}=10^6-10^7$. The plot of the internal energy as a function of the specific volume v for T_2 displays a kink and for T_3 a discontinuity, which is related to the gas–liquid phase transition. The isotherms T_1 and T_2 of the specific heat have strong maxima at $v=10^3$, resulting from the transition from the weak-correlation region (the Debye region) to the region of electroneutral ion triplets $(-1,+2,-1)$. In model 1 this transition corresponds to the transition to the region of large two-particle correlations (ion pairs).

The presence of structural transitions is confirmed by analysis of the radial distribution functions $g_{++}(r)$,

TABLE I. Comparative equilibrium properties of a small system consisting of 36 ions (v,u,Φ) and macroscopic properties[91] (v',u',Φ') in model 2 calculated per ion along the supercritical isotherm $T_1=0.287$ [here u is the specific internal energy (without the kinetic part), Φ is the compressibility factor, and p is the pressure].

lg p	lg v'	lg v	$-u'$	$-u$	Φ'	Φ
−5,35	3,80	—	0,072	0,195	0,98	—
−4,35	3,75	4,4	0,208	0,202	0,88	3,9
−3,35	2,66	3,04	0,450	0,323	0,72	1,70
−2,75	2,01	2,40	0,622	0,489	0,64	1,57
−2,23	1,47	1,80	0,775	0,637	0,60	1,30
−1,85	1,13	1,41	0,884	0,750	0,67	1,28
−1,35	0,73	0,99	1,01	0,887	0,84	1,52
−0,75	0,43	0,80	1,19	0,999	1,70	3,96
−0,35	0,26	0,47	1,26	1,079	2,80	4,62

$g_{+-}(r)$, and $g_{--}(r)$. On the high-temperature isotherm T_1 for $v=5\cdot10^2$ a maximum forms in $g_{--}(r)$ at the point $r=2$, which corresponds to the formation of ion triplets with linear structure; the positions of the triplets themselves are weakly correlated. In the liquid-density approximation linear triplets are deformed: the maximum in $g_{--}(r)$ is shifted toward large separations and broadens. At densities above the critical value correlations between doubly-charged ions are enhanced at a distance $r=2$, which corresponds to the continuous transition to a liquid in the chain structure. After the temperature is lowered the structuring processes appear more clearly on the T_2 isotherm, and the maximum in the radial distribution function becomes narrower and higher. Close to the critical density multiparticle associates appear in the form of ion chains, although the role of ion triplets remains dominant. The transition from the triple correlations to liquid correlations on the subcritical isotherm T_3 occurs discontinuously. The behavior of the function $g_{++}(r)$ at liquid densities implies that substructures of doubly-charged ions are present.

Ion clusters in a charge-symmetric 1–1-valent ion system have been studied in detail by the Monte Carlo method in Refs. 94 and 95, in the harmonic approximation in Refs. 96 and 97, by the Monte Carlo method in the generalized statistical ensemble in Ref. 98, and by the methods of the theory of physical groups in Refs. 89 and 90. A broad range of thermodynamic conditions is included in these calculations, from the formation of ion pairs in the gas phase to microcrystallization. The main results of these studies reduce to the following. The strong screening in a nonideal 1–1 ion system makes the long-range Coulomb potential effectively short-range. The smoothing of the long-range forces causes the properties of a small ion system to approach the corresponding properties of the macrophase. All types of restructuring that take place in the macrosystem are also observed in systems consisting of several dozen ions, and they occur at practically the same temperatures as in the macrosystem. For comparison it suffices to note that in systems of electroneutral particles with a Lennard–Jones interaction potential a cluster of 16 particles undergoes microcondensation at a temperature lower by a factor of two and microcrystallization at a temperature lower by a factor of three than in the macrosystem.[99] The absence of a delay in forming microdroplets in a cooled ionic system makes it impossible to reach a supersaturated ion plasma in which metastable thermodynamic states develop. The nucleate of the dense phase in an ion plasma has a chain structure: branching ion chains form from ions with alternating signs of the charge $(+-+-+-...)$. The closing of the chains into a compact structure is unfavorable from the entropic point of view, while dissociation is energetically unfavorable. The linear structure of the chain clusters causes the free energy of the ion microdroplets to have an extensive behavior (as in a macrosystem), and they grow in size without any phenomenon like nucleation of the critical size. These results for a 1–1-valent ionic system at first appeared to be universal for charged-particle systems, but as shown by subsequent studies to which the original part of the present paper is devoted, the loss of charged symmetry drastically changes the behavior of the ion system.

TABLE II. The same as in Table I, along the critical isotherm $T_2=0.125$.

lg p	lg v'	lg v	$-u'$	$-u$	Φ'	Φ
−5,05	3,94	3,9	0,830	0,60	0,62	0,6
−3,85	2,54	2,96	0,976	0,74	0,40	1,0
−3,35	1,67	2,55	1,07	0,84	0,17	0,9
−2,75	1,20	1,97	1,13	0,97	0,23	1,3
−2,23	0,65	1,63	1,20	1,01	0,21	2,0
−1,87	0,53	1,30	1,24	1,07	0,37	2,8
−1,35	0,39	1,54	1,30	1,10	0,87	12,5

TABLE III. The same as in Table I, along the subcritical isotherm $T_3 = 0.072$.

lg p	lg v'	lg v	$-u'$	$-u$	Φ'	Φ
−6,35	5,07	4,24	0,809	0,810	0,73	0,10
−5,35	3,74	3,94	1,097	0,817	0,34	0,53
−4,75	2,80	3,42	1,129	1,00	0,20	0,67
−4,35	0,41	3,04	1,366	0,89	0,0016	0,68
−2,75	0,35	1,33	1,392	1,27	0,056	1,0
−1,87	0,31	0,85	1,401	1,22	0,38	1,4

CALCULATION FOR A 2–1 VALENT SMALL ION SYSTEM BY THE MONTE CARLO METHOD

As noted above, the thermodynamic behavior of a 1–1-valent small ionic system differs little from the behavior of a 1–1 macrosystem even when the former contains only a few dozen ions. Whether the formation of an equilibrium microdroplet in a 2–1 system lags the condensation of the macrophase with formation of metastable states depends on whether the short-range nature of the shielded Coulomb potential is effectively maintained when the charged symmetry of the system is destroyed. To clarify this matter we have carried out calculations by means of the Monte Carlo method in the present work using the NpT statistical ensemble of equilibrium thermodynamic properties of a small 2–1-valent ionic system consisting of 36 ions with the charged-sphere model at the same p, T points as in Ref. 91. In addition to this we have calculated the $T_4 = 0.05$ low-temperature isotherm lying far below the critical point of

the model macrosystem. The system is situated in a spherical cavity with a variable radius that acts as a spherical piston. These boundary conditions duplicate the conditions used to model the problem in Ref. 95. The center of mass of this system is not fixed. When the Markov chain is generated the (36×36) energy matrix is stored in the computer memory, speeding up the process of calculation by a factor of 1.5–2. The Markov process is directed by the transition probability matrix, which satisfies the condition of detailed balance: $W_{ij}/W_{ji} = \exp[-(U_i - U_j)/kT]\exp[-p(V_i/V_j)/kT]$, where i and j are configurations with energy U_i, U_j and volume V_i, V_j, respectively.

Tables I–V display the results of the Monte Carlo calculations carried out in the present work for a 2–1-valent small system of charged spheres. In Figs. 1 and 2 these results are compared with the data[91,92] on the modeling of a macroscopic system. On the $T_1 = 0.287$ high-temperature isotherm the difference in the values of the internal energy

TABLE IV. The same as in Table I, along the subcritical isotherm $T_4 = 0.050$.

lg p	lg v	$-u$	Φ
−5,88	3,95	1, 00	0,5
−5,35	3,63	1,02	0,3
−4,92	3,34	1,09	0,5
−4,44	3,26	1,10	1,3
−3,96	2,76	1,11	1,2
−3,49	2,47	1,17	2,0
−2,54	1,27	1,28	1,1
−2,06	0,43	1,35	0,5
−1,59	0,17	1,37	0,8

TABLE V. Normalized density distribution of a small system (36 ions) as a function of distance from the center of mass for different values of the pressure p and subcritical temperature $T_4 = 0.050$.

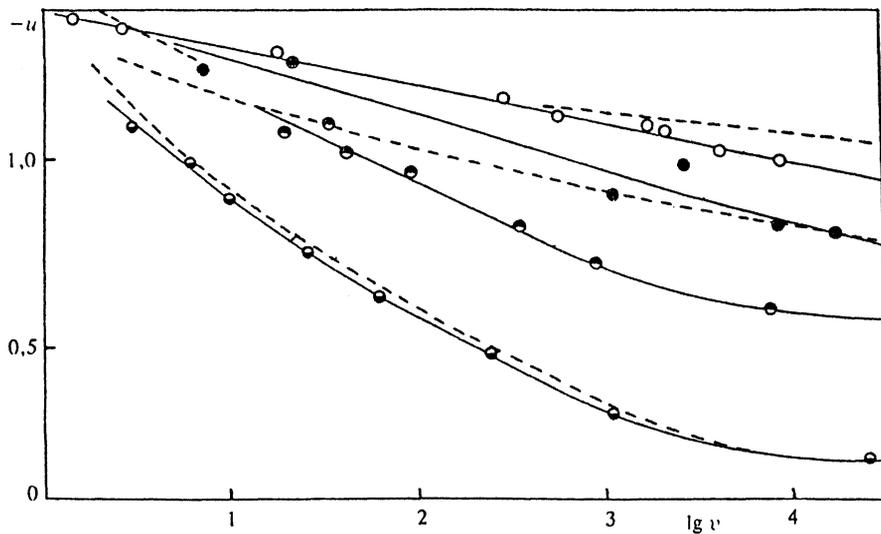| R	$p \cdot 10^3$		
	0,108	0,968	8,72
0,19	0	0	0
0,76	0	0	0,43
1,33	0	0	0,65
1,90	0	0,0013	0,58
2,47	0	0,0098	0,25
3,04	0	0,025	0,045
3,61	0	0,048	0
4,18	0	0,060	0
4,75	0,0006	0,059	0
5,32	0,0011	0,042	0
5,89	0,0035	0,012	0
6,46	0,0076	0,0008	0
7,03	0,011	0	0
7,60	0,012	0	0
8,17	0,013	0	0
8,74	0,015	0	0
9,31	0,016	0	0

FIG. 1. Specific internal energy [without the kinetic part $(3/2)kT$] as a function of the specific volume in a system of hard spheres without charge symmetry (model 2): ◒—$T=0.287$, ●—$T=0.072$, ◓—T $=0.125$, ○—$T=0.050$. The solid traces and points correspond to the small system with 36 ions, the dashed curves correspond to the macrosystem using the data of Ref. 91. Calculation done using the Monte Carlo method.

of the small system and the macroscopic system are of the same order as for the 1–1 system in the weak-correlation region. The density of the small system is found to be several times less than that of the macrosystem at the same pressure. The compressibility factor of the small system (Table I) becomes larger than unity even at a density two to three times less than liquid densities, while in the macrosystem it crosses the unit level only when the system is compressed up to liquid densities. The radial distribution function data[91] show that in this density range notable three-particle correlations are exhibited, which we associated with the increase in the compressibility factor Φ in the small system. The data[95] show that the compressibility factor of a small 1–1-valent system approaching liquid densities passes through a minimum with a value less than unity, i.e., it behaves qualitatively just like a macrosystem. In the 2–1-valent small system the compressibility factor grows monotonically as a function of density in the density region 10^0–10^{-5}; there is no minimum (see Table I and Fig. 2).
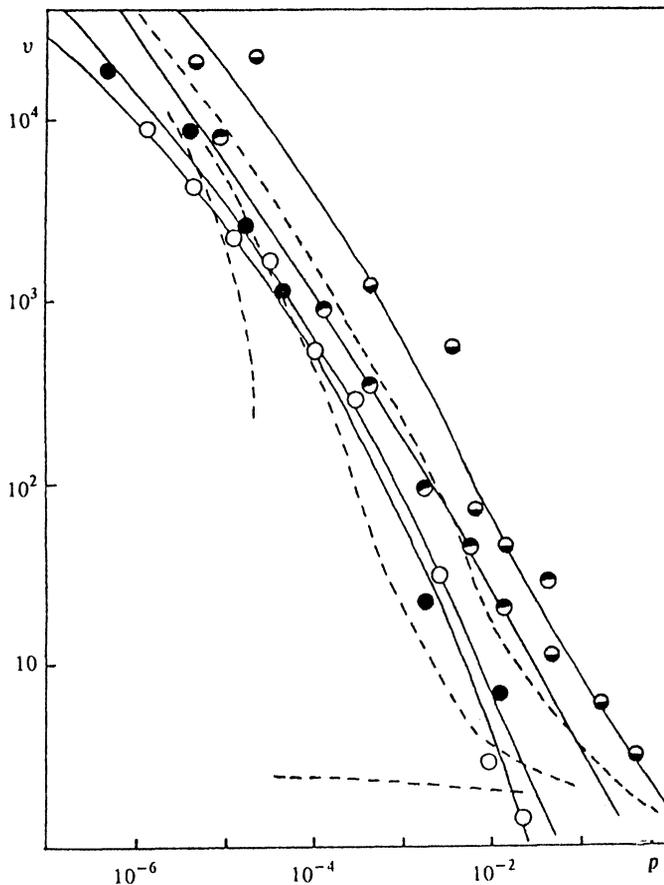

FIG. 2. Equation of state for a system of hard spheres without charge symmetry (model 2): ◒—$T=0.287$, ●—$T=0.125$, ◓—T $=0.072$, ○—$T=0.050$. Here the solid traces and points correspond to the small system consisting of 36 ions, and the dashed curves are for the macrosystem using the data of Ref. 91. Calculation performed using the Monte Carlo method.
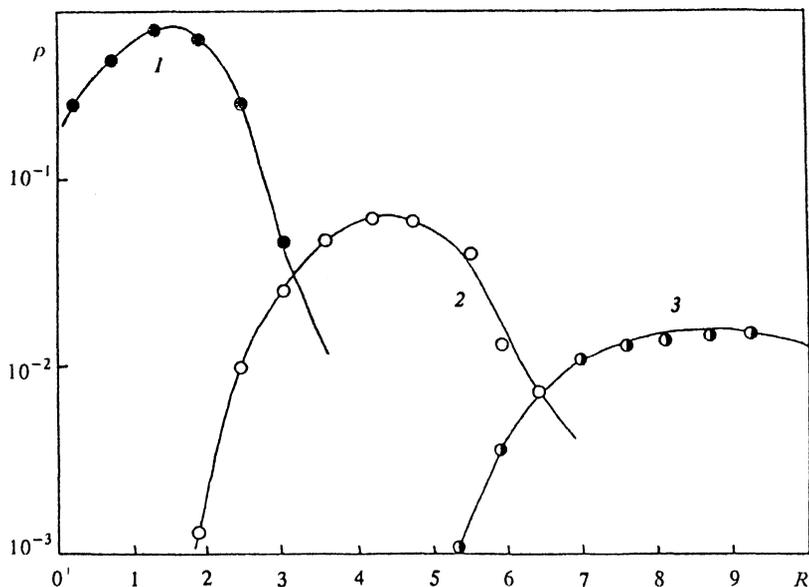
FIG. 3. Density profile in a system of 36 ions (model 2) as a function of distance from the center of mass for $T=0.05$: 1) $p=8.72 \cdot 10^{-3}$; 2) $p=0.968 \cdot 10^{-3}$; 3) $p=0.108 \cdot 10^{-3}$. Calculation performed using the Monte Carlo method.

The internal energy of the small system changes monotonically along the $T_2=0.125$ isotherm. The deviation toward larger values in comparison with the macroscopic at the same density grows as the density decreases from a few to a several times ten percent ($\sim kT$). The substantial difference in the values of the internal energy between the small system and the macrosystem at low densities is due here to the deflection of the macrosystem isotherm, which was attributed by Shiff[91] to the closeness of the critical point, i.e., to the rise in the multiparticle correlation revealed in the radial distribution function. In the small system this deflection is observed only in the next, lower-temperature isotherm T_3. The delay in initiating the multiparticle correlations in the small system, as will be clear from the discussion below, is related to the internal repulsive forces and the enhanced values of the compressibility factor in the small system. Compression to specific volumes of order $v=10^{+1}$ leads to equalization of the internal energies of the small system and the macrosystem, since the Coulomb forces at such densities become weaker than the short-range hard-sphere repulsion, and the absence of charge symmetry in the system assumes secondary importance. The radial distribution functions $g_{++}(r)$ and $g_{--}(r)$ in the macrosystem[91] at these densities exhibit equalization of the heights of the first maxima at the distance $r=2$, and the correlation length decreases to $r=2.5$, i.e., it becomes smaller than the linear dimensions of the small system.

In the equation of state, Fig. 2, for $\rho > 10^{-2}$ the density of the small system is an order of magnitude smaller than that of the macrosystem, while for small $\rho (<10^{-2})$ they agree satisfactorily, i.e., the difference in densities behaves in just the opposite way from the difference in energies. The difference in energies for equal specific volumes ($\rho < 10^{-2}$) implies that the multiparticle correlations are primarily orientational near the critical point. Analysis of the ionic configurations in the system shows that these are orientational correlations of linear ion triplets ($-+-$). For small system volumes, when the dimensions of the

small system become comparable with those of an ion triplet, even a slight delay in the orientational correlations, which has little effect on the energy, significantly increases the volume and loosens up the system. The compressibility factor (Table III) intersects the $\Phi=1$ level even for $\rho=10^{-3}$, when the average distance between particles is of the order of ten ion diameters. The repulsive interaction at such distances cannot be ascribed to the short-range part of the charged-sphere potential, and is related to the Coulomb interaction. In the macrosystem the level $\Phi=1$ is reached only at liquid densities. In the single-particle distribution function, measured from the center of mass of the small system, a gap develops in the neighborhood of the center of mass as liquid densities are approached. The abrupt decrease in the density in the center of the small system is due to the internal repulsive forces. As the temperature decreases (Fig. 3) the density in the center decreases by several orders of magnitude; in fact a cavity develops with no particles inside.

The $T_3=0.072$ isotherm in the macrosystem intersects the gas–liquid coexistence curve: the specific volume changes discontinuously by more than two orders of magnitude from 10^3 to a few times unity, and the compressibility factor decreases discontinuously from 0.20 to 0.0016. In the gaseous phase the radial distribution function and the instantaneous ion configurations clearly display the formation of ion triplets. The phase transition is immediately preceded by an abrupt rise in the correlations of the doubly-charged ions at a distance of two diameters, which corresponds to "merging" of ionic triplets. In the small system the compressibility factor (Table III) at the phase transition point in the macrosystem continues to grow monotonically, intersecting the unit level, and differs here from the macrosystem by more than a factor of one hundred. If the specific volumes of the small system and the macrosystem have the same order of magnitude on the gaseous branch of the equation of state, then at a pressure $p=10^{-4}$ the macrosystem has a typically liquid density, while the small system remains in a gaseous state. The

compressibilities $\varkappa_T = -\partial(\ln v)/\partial p$ are determined from the slopes of the curves, and differ here by a factor of twenty. In a time sequence of configurations of the small ionic system individual ion triplets are visible.

The ion binding energy in a geometrically regular ion triplet is -1.16 per particle in the calculation. Even when the densities approach that of the liquid state the internal energy of the small system decreases by less than 5% from this value, which implies that the orientational correlation of the triplets is weak. The corresponding binding energy of the correlations in the macrosystem is larger by a factor of three. The phase transition in the macrosystem is accompanied by a transition from the energy of the ion triplets to much lower values (Fig. 1). The size of the cavity that forms in the center of the small system under stable liquid macrophase conditions, which is equal to several ion diameters, yields an estimate for the distances over which the potential of the average force between ionic triplets, averaged over the mutual orientations, is repulsive.

From the general theory of capillarity it is well known that owing to surface effects the formation of a dense phase encounters difficulty in a small system and usually occurs for more intense cooling and stronger compression than in a macrosystem. One can speak conditionally about a "coexistence curve" and "critical point" for the small system, whose positions depend on the number of particles. Here we must keep in mind that the very concept of a "phase transition" in a system with a bounded number of particles is problematical.[40] The T_3 isotherm on the pV diagram has a discontinuity for the macrosystem and is found to be continuous for the small system. For every subcritical temperature, generally speaking, there exists a minimum size of the nucleate which may become critical, i.e., remain in equilibrium with the gas at the corresponding pressure. Each size has its own coexistence curve with the dense microphase, tangent to the given subcritical isotherm of the small system in the region of metastable states of the macrosystem. From these results obtained by simulating the small system it follows that the coexistence curve for $N=36$ lies below the isotherm of the $T_3=0.072$ metastable states, i.e., the minimum size of the nucleate for this temperature is larger than $N=36$. A further decrease in the temperature to $T_4=0.050$ (Fig. 2) did not bring about the discontinuous formation of a microdroplet like that which took place in the charged-symmetric 1–1-valent small ionic system.[95] The isotherm has the smooth form typical of the gaseous phase (Fig. 2). In the center of the system a cavity develops, which remains also at the highest pressure (Fig. 3). The compressibility factor passes through a minimum greater than unity (Table IV).

ESTIMATES OF THE EQUILIBRIUM ION-PAIR AND TRIPLET CONCENTRATIONS IN A SYSTEM WITHOUT CHARGE SYMMETRY

The results of simulating a 2–1-valent ionic system imply that, as in the 1–1 system, the formation of stable ion associates is the decisive factor in determining the equilibrium properties of highly nonideal plasmas. The internal repulsive forces in an ion microdroplet in model 2, as will

be shown in detail in the next section of the present paper, are caused by the interaction of the ion triplets.

The results and the method of calculating the equilibrium ion cluster densities in Refs. 89 and 90 cannot be transferred without change to model 2 since in Refs. 89 and 90 substantial use was made of the condition that the anions and cations had equal activities $z_{\pm} = \Lambda_{\pm}^{-3} \exp(\mu_{\pm}/kT)$, where $\Lambda_{\pm} = h(2\pi m_{\pm} kT)^{-1/2}$ is the thermal de Broglie wavelength. The activity can be expressed in terms of the configuration integral $Z(N_+, N_-, V, T)$ of the system and does not depend on the particle mass:

$$z_{\pm} = \exp\left[-\frac{\partial \ln[Z(N_+, N_-, V, T)]}{\partial N_{\pm}}\right] \exp\left[\frac{\partial \ln(N_{\pm}!)}{\partial N_{\pm}}\right].$$

(1)

The symmetry condition (1) with respect to charge conjugation is satisfied when the numbers of anions and cations are the same, $N_+ = N_-$, and the diameters and valences of the ions are equal without being scaled by the masses. In the 2–1 system we have $z_+ \neq z_-$, where the relation between z_+ and z_- changes as the temperature and density vary.

We write down the usual expression for the statistical sum of an n-component system in the macrocanonical ensemble:[41]

$$\Omega(\{\lambda_i\}, V, T) = \sum_{\{K_i\}} Q(\{K_i\}, V, T) \prod_i \lambda_i^{K_i},$$

(2)

where $\{K_i\} \equiv (K_1, K_2, ..., K_n)$ is the composition, $\lambda_i = \exp(\mu_i/kT)$ is the absolute activity, μ_i is the chemical potential of the ith component, and $Q(\{K_i\}, V, T)$ is the canonical integral of the system with composition $\{K_i\}$. We represent the integral $Q(\{K_i\}, V, T)$ in the form of a sum of integrals over the regions of phase space, to each of which we associate a subdivision of the system into physical groups (clusters), determined by the infinite n-dimensional tableau $\|N\|$ with elements $N_{\{k_i\}}$, a collection of composition groups $\{k_i\} = (k_1, k_2, ..., k_n)$:

$$Q(\{K_i\}, V, T) = \sum_{\substack{\sum_{\{k_i\}} k_i N_{\{k_i\}} = K_i}} Q(\|N\|, V, T).$$

(3)

Then (2) can be written in the form

$$\Omega(\{\lambda_i\}, V, T) = \sum_{\{K_i\}} \left(\sum_{\substack{\sum_{\{k_i\}} k_i N_{\{k_i\}} = K_i}} Q(\|N\|, V, T) \prod_i \lambda_i^{K_i} \right)$$

$$= \sum_{\|N\|} Q(\|N\|, V, T) \prod_{\{k_i\}} \prod_i \lambda_i^{k_i N_{\{k_i\}}}$$

$$= \sum_{\|N\|} Q(\|N\|, V, T) \prod_{\{k_i\}} \lambda_{\{k_i\}}^{N_{\{k_i\}}},$$

(4)

where $\Sigma_{\|N\|}$ represents summation over all possible n-dimensional infinite tableaux $\|N\|$ with nonnegative

whole-number elements, and $\lambda_{\{k_i\}} = \Pi_i \lambda_i^{k_i}$ is the absolute activity of the composition group $\{k_i\}$. The relations (2)–(4) are exact. In the approximation of independent physical groups

$$Q(\|N\|, V, T) \approx \prod_{\{k_i\}} \frac{1}{N_{\{k_i\}}!} (q_{\{k_i\}})^{N_{\{k_i\}}}, \qquad (5)$$

where $q_{\{k_i\}}$ is the statistical integral of the composition group $\{k_i\}$. In this approximation (4) simplifies considerably:

$$\Omega(\{\lambda_i\}, V, T) = \sum_{\|N\|} \prod_{\{k_i\}} \left(\frac{1}{N_{\{k_i\}}!} q_{\{k_i\}}^{N_{\{k_i\}}} \right) \prod_{\{k_i\}} \lambda_{\{k_i\}}^{N_{\{k_i\}}}$$

$$= \prod_{\{k_i\}} \sum_N \frac{1}{N!} (q_{\{k_i\}})^N \lambda_{\{k_i\}}^N$$

$$= \prod_{\{k_i\}} \exp(q_{\{k_i\}} \lambda_{\{k_i\}}) \qquad (6)$$

or

$$\ln \Omega(\{\lambda_i\}, V, T) = \sum_{\{k_i\}} q_{\{k_i\}} \lambda_{\{k_i\}}. \qquad (7)$$

Differentiating (7) with respect to $\ln(\lambda_{\{k_i\}})$ we find the equilibrium concentration of the composition groups $\{k_i\}$:

$$\rho_{\{k_i\}} = \frac{\lambda_{\{k_i\}}}{V} = \frac{\partial \ln \Omega(\{\lambda_i\}, V, T)}{\partial \lambda_{\{k_i\}}}$$

$$= \frac{q_{\{k_i\}}}{V} \lambda_{\{k_i\}} = \frac{x(\{k_i\})}{V} z_{\{k_i\}}, \qquad (8)$$

where $x(\{k_i\}) = \Pi_i(\Lambda^3)^{k_i} q_{\{k_i\}}$ is the configuration integral and $z_{\{k_i\}} = \Pi_i(\Lambda^{-3})^{k_i} \lambda_{\{k_i\}}$ is the activity of the composition group $\{k_i\}$. If the momenta do not enter into the definition of a group, then $z_{\{k_i\}}$ contains integration only over configuration space and does not depend on the ion masses. The independence of $z_{\{k_i\}}$ on the masses follows from expression (1). Equations (3)–(8) remain valid for any definition of a cluster. In order to go over to numerical estimates we must specialize to a cluster definition. We will use the term "cluster" to mean a connected diagram of ions with negative interaction energy, where two particles are assumed to be coupled if the distance between them is less than R_m and they have different signs.

Analysis of the radial distribution functions obtained by the Monte Carlo method[91,92] reveals that in the region immediately adjacent to the gas–liquid coexistence curve, on the side of low densities and high temperatures, highly developed three-particle correlations are observed—the system is organized into a gas made of electroneutral ion triplets. Then the equilibrium densities of the larger associates at densities less than liquid density are negligibly small:

$$\gamma \equiv (\rho - \rho_1^+ \rho_2^- - 2\rho_2 - 3\rho_3)/\rho \ll 1, \qquad (9)$$

where $\rho = v^{-1}$ is the molar density of the macrosystem and ρ_n is the molar equilibrium density of n-ion clusters. We find expressions for ρ_1^+, ρ_1^-, ρ_2, and ρ_3 in zeroth order in the small parameter γ. For this purpose we use (8) to write down relations for the density:

$$\frac{\rho_3}{(\rho_1^-)^2 \rho_1^+} = \frac{x_3/V}{(x_1^-/V)^2(x_1^+/V)} = x_3/V,$$
$$\frac{\rho_2}{\rho_1^+ \rho_1^-} = \frac{x_2/V}{(x_1^-/V)(x_1^+/V)} = x_2/V, \qquad (10)$$

where $x_1^+ = x(1,0) = V$, $x_1^- \equiv x(0,1) = V$, $x_2 \equiv x(1,1)$, $x_3 \equiv x(1,2)$ are configuration integrals of monomers, ion pairs, and triplets. Setting $\gamma = 0$ we can write down the conditions for conservation of the number of ions of each species:

$$\rho_1^+ + \rho_2 + \rho_3 = \rho/3,$$
$$\rho_1^- + \rho_2 + 2\rho_3 = 2\rho/3. \qquad (11)$$

The real positive solution of the system of four equations (10), (11) for ρ_1^-, ρ_1^+, ρ_2, and ρ_3 has the form

$$\rho_1^- = \sqrt{a}\left[\cos\left(\frac{\varphi}{3}\right) + \sqrt{3}\sin\left(\frac{\varphi}{3}\right)\right] - \frac{x_2/V}{x_3/V},$$

$$\rho_1^+ = \frac{\rho}{3[1 + (x_2/V)\rho_1^- + (x_3/V)(\rho_1^-)^2]}, \qquad (12)$$

$$\rho_2 = (x_2/V)\rho_1^+ \rho_1^-, \quad \rho_3 = (x_3/V)\rho_1^+ (\rho_1^-)^2,$$

where

$$\varphi = \arctan\left(\sqrt{a^3/b^2} - 1\right),$$

$$a = \frac{1}{9}\left(\frac{x_2/V}{x_3/V}\right)^2 - \frac{1 - \rho(x_2/V)/3}{3(x_3/V)}, \qquad (13)$$

$$b = \left[\frac{x_2/V}{3(x_3/V)}\right]^3 - \frac{(x_2/V)[1 - \rho(x_2/V)/3]}{6(x_3/V)^2} - \frac{\rho}{3(x_3/V)}.$$

The ion-ion potential in model 2 gives rise to integrals which are not expressible in terms of elementary functions when we evaluate the configuration integrals x_2 and x_3 in Eq. (12). These are the integral logarithm and its integrals. The Coulomb-potential approximation by means of the function $u^-(R) = -2(1 - \ln R)$ avoids this difficulty. On the domain of integration $1 < R < R_m$ for $1 < R_m < 1.1$ the function $u^-(R)$ differs from the Coulomb potential $-2/R$ by less than 0.4% ($\sim 0.1kT$). For x_2 we find

$$x_2 = V \int_1^{R_m} 4\pi R^2 \exp[-2(-1 + \ln R)/T] dR$$

$$= \frac{4\pi V}{3 - 2/T} [R_m^{(3 - 2/T)} - 1] \exp\left(\frac{2}{T}\right). \qquad (14)$$

In evaluating x_3 in the approximation $R_m - 1 \ll 1$ we assume that the distances between the ions are equal to $2\sin(\alpha/2)$, Fig. 4. The Coulomb repulsive potential of the B and C ions on the interval $1 < R < 2$ is approximated to within 8% ($\sim kT$) by the function $u^*(R) = (3 - R)/2$. Since the error in the approximation is less than 2% in comparison
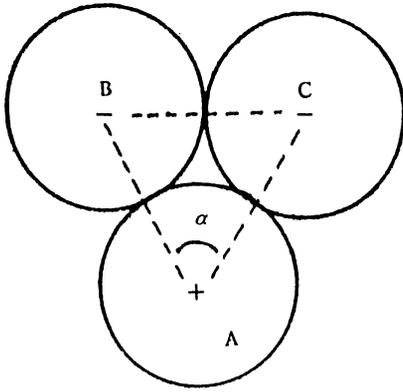
FIG. 4. Diagram of an ion triplet.

with the total energy of the ion triplet, the temperature shift in the functions resulting from this approximation is only a few percent, which is quite acceptable for our approximate estimates.

$$x_3 = V\left\{ \int_1^{R_m} 4\pi R^2 \exp\left[\frac{2(1-\ln R)}{T}\right]dR \right\}^2$$

$$\times \frac{1}{2} \int_{\pi/3}^{\pi} \sin(\alpha)\exp\left[-\frac{3-2\sin(\alpha/2)}{2T}\right]d\alpha$$

$$= \frac{x_2^2}{2V}\exp\left(-\frac{3}{2T}\right)\cdot 4T^2 \int_{2/T}^{1/T} \tilde{x}\exp(\tilde{x})d\tilde{x}$$

$$= \frac{x_2^2}{V}2T^2\left[\exp\left(-\frac{1}{2T}\right)\left(\frac{1}{T}-1\right)-\exp\left(-\frac{1}{T}\right)\left(\frac{1}{2T}-1\right)\right].$$

(15)

In the second relation (15) we have changed the integration variable to $\tilde{x}\equiv\sin(\alpha/2)/T$.

It is easy to see that Eqs. (9)–(13) allow us to construct a numerical iteration procedure for determining the higher-order corrections in γ to Eqs. (12).

Figure 5 shows the results of a numerical calculation of the relative ion-pair, triplet, and monomer concentrations versus the temperature according to Eqs. (12)–(15). The
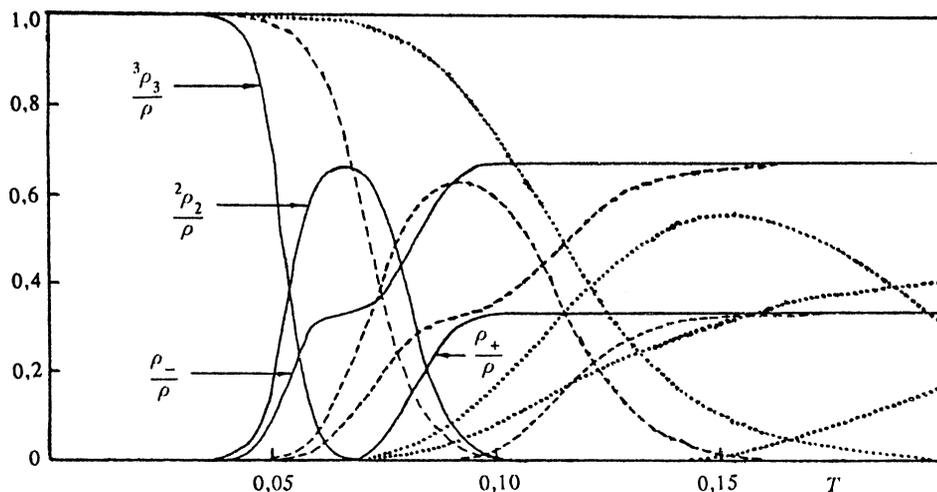
ion-pair concentration passes through a maximum near the start of the rise in ion triplet concentration. For low densities ($\rho < 10^{-6}$) the fraction of particles trapped in ion pairs reaches a saturated value $2\rho_2 = 2\rho/3$ somewhat earlier than the formation of triple associates begins. Its formation requires an additional negative ion. Consequently, free negative ions are lost more slowly as the system is cooled, as can be seen from the deflection in the temperature dependence of ρ_1^- near the extremum of ρ_2. As the temperature decreases further the system is converted entirely into a gas of ion triplets. At high densities ($\rho > 10^{-6}$) the deflection of ρ_- is smoothed out, since the ion triplets begin to form before all of the positive doubly-charged ions become trapped by ion pairs—the extremum of ρ_2 does not reach its saturated value. As the system becomes denser the region of pure pair correlation becomes partly absorbed by the triplet correlation region, and disappears in the approach to the critical density. In Fig. 6 the same quantities are shown as functions of the specific volume of the system.

The formation of larger associates out of electroneutral triplets leads to a slight decrease in the energy and therefore does not grow much for temperatures below critical. However, on the superthermal isotherms along with the disappearance of the phase transition the mechanism for formation of the liquid phase through triplet ion association also disappears, since as the temperature increases the role of the Coulomb part of the potential is smoothed out in comparison with the short-range repulsion.

Figure 7 displays contour levels for the fraction of particles trapped in ion triplets on the V-T plane, calculated from relations (12)–(15).

POTENTIAL OF THE AVERAGE FORCE IN THE LATTICE APPROXIMATION FOR INTERACTING ION ASSOCIATES

Since the 2–1-valent ion system is organized into a gas of ion triplets in the immediate vicinity of the transition to the dense phase (Fig. 7), we must look at the behavior of the latter interaction for a reason for the anomalous behavior of the small ionic system when the symmetry of the charged components is violated.
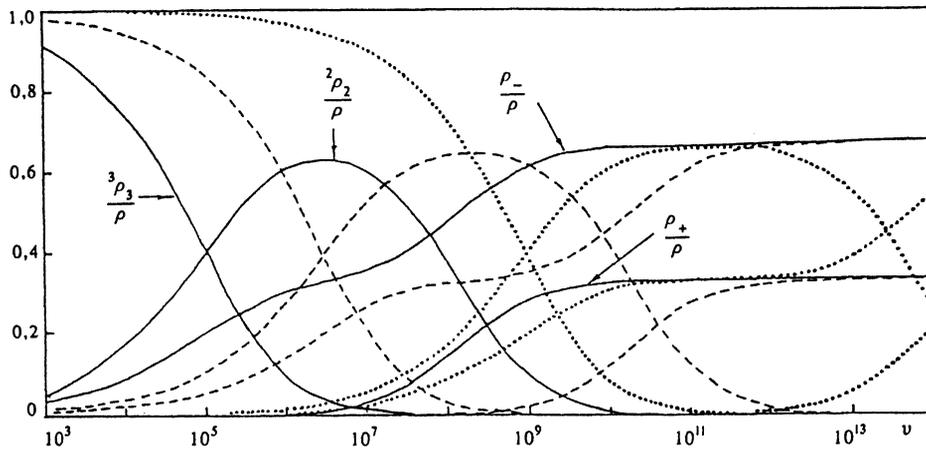

FIG. 5. Temperature dependence of the equilibrium densities ρ_3 of ion triplets, ρ_2 of ion pairs, and $\rho_+ \equiv \rho_1^+$, $\rho \equiv \rho_1^-$ for monomers in a system of hard spheres without charge symmetry (model 2), calculated using Eqs. (12)–(15) for various gross molar densities: dotted curves) $\rho = 10^{-4}$; dashed curves) $\rho = 10^{-7}$; solid curves) $\rho = 10^{-10}$ with $R_m = 1.1$. The independent-cluster approximation was used.

FIG. 6. Equilibrium densities ρ_3 of ion triplets, ρ_2 of ion pairs, and ρ_+, ρ_- of monomers in a system of hard spheres without charge symmetry (model 2) as a function of the specific gross volume calculated according to Eqs. (12)–(15) for different temperatures: solid traces) $T=0.1$; dashed traces) $T=0.08$; dotted traces) $T=0.06$, for $R_m=1.1$. The independent-cluster approximation was used.

The relative orientation of two linear triplets is characterized by the direction of the vector $\mathbf{r}$ connecting the centers of mass of the triplets and the vectors $\mathbf{r}_1$ and $\mathbf{r}_2$ which coincide with the axes of symmetry of the triplets. Consider the discretized space of mutual orientations of linear ion triplets, a space consisting of configurations in which the axes of symmetry of the latter can be either parallel or mutually orthogonal. Equal phase volumes are assigned to all configurations. Each of the vectors $\mathbf{r}$, $\mathbf{r}_1$, and $\mathbf{r}_2$ in these configurations can be directed in six ways, parallel to one of the three Cartesian axes. Thus, the discrete space of the joint orientations contains $6 \times 6 \times 6 = 720$ states. It suffices to specify $\mathbf{r}_1$ and to consider $6 \times 6 = 36$ configurations, since only the relative orientation of the triplets is important. In four of the 36 configurations the triplet axes lie on one straight line, in eight configurations they are parallel but lie on different straight lines, in eight the axes are mutually perpendicular and lie on different planes, and in 16 they lie in a single plane. When we average the interaction energy of randomly oriented triplets the weights assigned to these four types of orientation are in the proportion 1:2:2:4. The dependence of the interaction energy on the distance between triplet centers for all four types of orientation is shown in Fig. 8. Only the fourth type of orientation gives rise to mutual attraction of the triplets; all the others give rise to repulsion. As can be seen from Fig. 8, the triplets repel on the average as $T \to \infty$. When the temperature is reduced the contribution from the energetically favorable orientations of the fourth type

increases, and the repulsion becomes an attraction. The result of the competition between the different orientations depends on the distance. Figure 9 displays plots of the interaction pseudopotentials of the ion triplets obtained by averaging in the discretized space over the reciprocal orientations with the Gibbs weights:

$$u_T(r) = \left\{ u_1(r)\exp\left[-\frac{u_1(r)}{kT}\right] + 2u_2(r)\exp\left[-\frac{u_2(r)}{kT}\right] \right.$$

$$+ 2u_3(r)\exp\left[-\frac{u_3(r)}{kT}\right] + 4u_4(r)\exp$$

$$\times \left[-\frac{u_4(r)}{kT}\right] \right\} \left\{ \exp\left[-\frac{u_1(r)}{kT}\right] + 2\exp \right.$$

$$\times \left[-\frac{u_2(r)}{kT}\right] + 2\exp\left[-\frac{u_3(r)}{kT}\right] + 4\exp$$

$$\left. \times \left[-\frac{u_4(r)}{kT}\right] \right\}^{-1}.$$ (16)

The repulsive character of the pseudopotential at intermediate distances becomes attractive at small distances, Fig. 9. At a distance r_m the maximum energy is reached. The probability of finding two ion triplets at a distance r is estimated by replacing the potential of the average force in the expression for the radial distribution function by the approximate pseudopotential
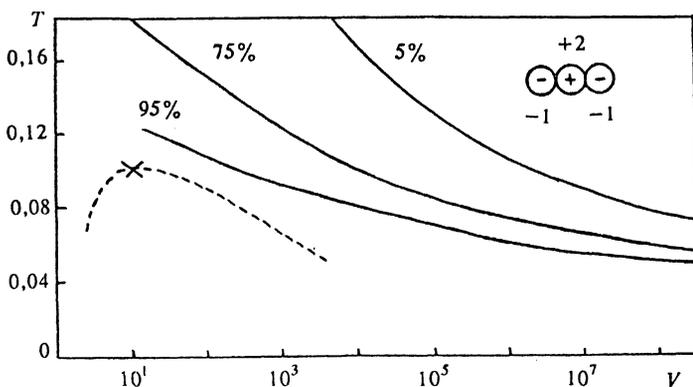

FIG. 7. Curves of constant relative ion-triplet molar content in a system of hard spheres without charge symmetry (model 2) on the phase diagram of the system. The numbers correspond to the molar fraction of the ions trapped in ion triplets. The calculation was done using the independent-cluster approximation. The broken trace represents the gas–liquid coexistence boundary in the macrosystem and $\times$ is the critical point.
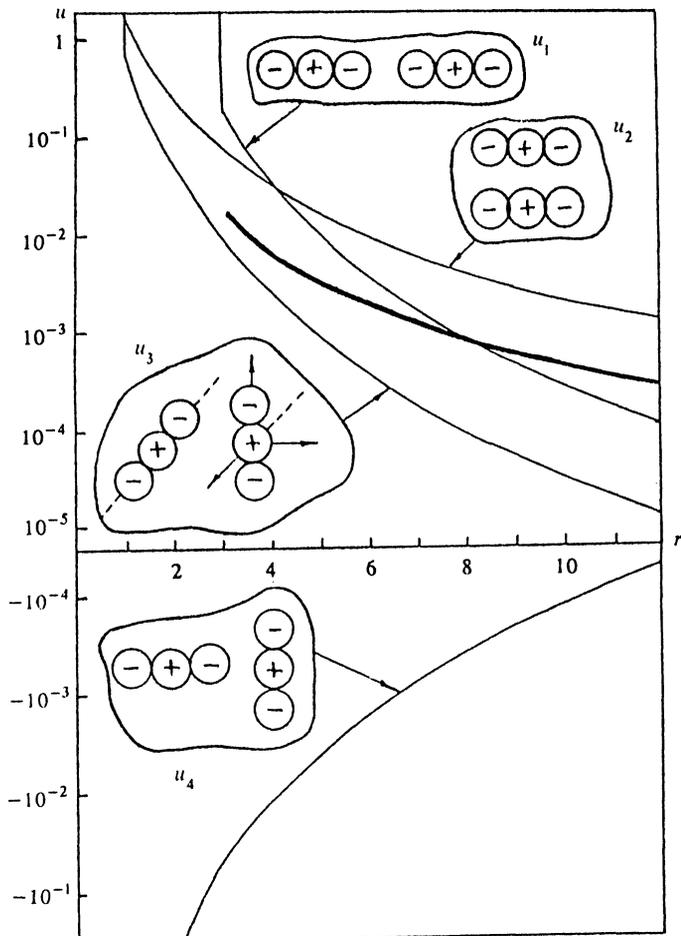
FIG. 8. Ion triplet interaction energy in the 2–1-valent ion system in various mutual orientations. Only one type of orientation corresponds to a negative energy and to attraction. The heavy line represents the energy averaged over all four types of orientation, corresponding to $T = \infty$.

$$G(r) = \exp[-u_T(r)/kT]. \tag{17}$$

This approximation is equivalent to neglecting three-particle and multiple interactions among the ion associates. The result of calculating (17) numerically is shown in Fig. 10. If the maximum of $u_T(r)$ decreases as the temperature decreases, then the associated minimum $G(r)$ deepens.

The relatively weak minimum of $G(r)$ has important consequences for the structure of the nucleating microscopic irregularities (microdroplets) with linear dimensions comparable to r_m. The fact that the width of this minimum is comparable with the dimensions of the irregularities makes these consequences even more significant.

The potential of the average resulting force exerted on an individual ion triplet by all other triplets, disregarding higher correlations among the ion associates, takes the form

$$W = \rho \int_0^\infty G(r) 4\pi r^2 [-kT \ln G(r)] dr. \tag{18}$$

The higher correlations among the ion triplets, on the one hand, must be taken into account in describing the interaction of an individual ion associate with microscopic irregularities in the system; on the other hand, taking into account the higher correlations entails corrections in the
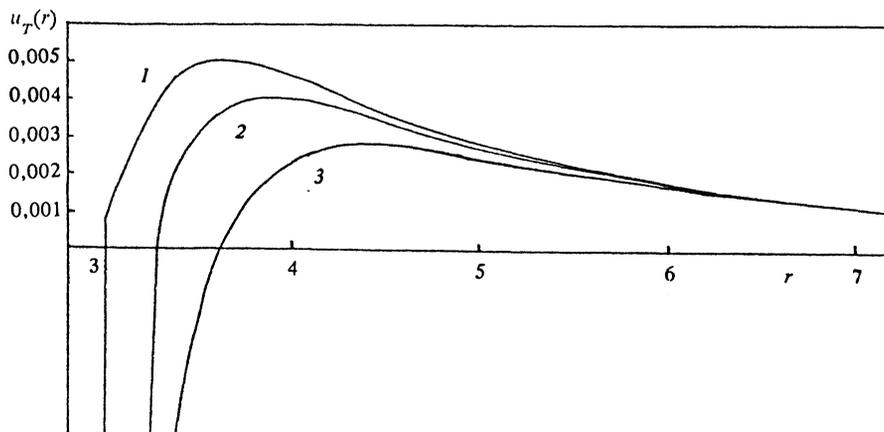

FIG. 9. Ion–triplet interaction pseudopotential obtained by averaging over the mutual orientations with the Boltzmann weight for different temperatures: 1) $T=0.3$; 2) $T=0.2$; 3) $T=0.1$.
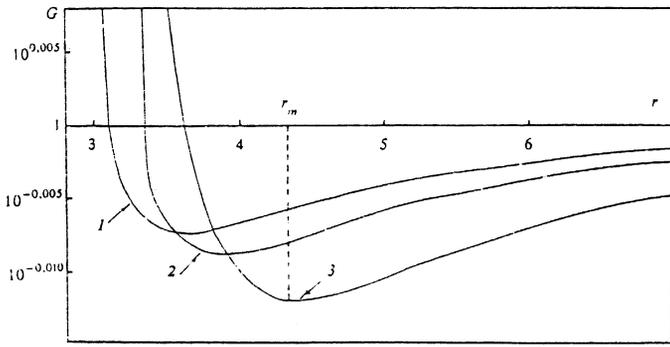
FIG. 10. Probability density for observing two clusters of three ions in model 2 at a distance r, normalized with respect to the volume. The ordinate is a logarithmic scale. The lattice approximation was used (1—$T=0.3$; 2—$T=0.2$; 3—$T=0.1$).

integrand of Eq. (18). It is well known from the general theory of integral equations for correlation functions[41] that an infinite chain of n-particle correlation functions g_n, $n=1,2,...,\infty$ represents a self-consistent set satisfying an infinite system of coupled integral equations (the Bogolyubov–Born–Green–Kirkwood–Yvon equations). Each of the functions g_n is expressed in terms of the following function g_{n+1} in the hierarchy. The infinite set of equations can be closed and converted to a finite system only approximately. An example is the well-known superposition approximation for g_3 (Ref. 41). In the spirit of these ideas about the functional relation between the lowest and highest correlations in the system it is easy to understand that the thermodynamic likelihood of formation in a system of microscopic irregularities must be imposed even in the form of the very lowest, binary correlations between ion associates. We can convince ourselves that when the specific form of $G(r)$ for ion triplets is included the formation of microscopic irregularities in the 2–1 ionic system is

thermodynamically favored, but instead of aiding nucleation their profile impedes it even in the initial stage.

Consider some virtual microscopic irregularity at a fixed distance from an isolated ion triplet, so that the average density of the system at a distance r from it differs by a factor $\theta(r)$ from the corresponding value for a triplet immersed in a uniform system. In this case the potential of an average force at the location of a triplet near the microscopic irregularity is

$$W' = \rho \int_0^\infty G(r)\theta(r)4\pi r^2[-kT \ln G(r)]dr. \quad (19)$$

The relative probability of finding a triplet at this point coupled to the microscopic irregularity is equal to

$$\exp\left(-\frac{W'-W}{kT}\right) = \exp\left\{\rho \int_0^\infty G(r)4\pi r^2 \ln G(r)\right.$$

$$\left. \times [\theta(r)-1]dr\right\} \approx G^M(r_m). \quad (20)$$

The last approximate expression is justified if the quantity $\theta(r_m)-1$ is sufficiently large that the principal contribution to the integral (20) comes from the neighborhood of the minimum of $G(r)$ at $r=r_m$, and M is the effective number of triplets that happen to be in the region of this minimum, defined as

$$M \equiv \frac{\rho}{\ln G(r_m)} \int_0^\infty G(r)\theta(r)4\pi r^2 \ln G(r)dr. \quad (21)$$

The ratio of the probabilities of finding an ion triplet at two separate points "1" and "2" near the microscopic irregularity can be estimated by the relation

$$[G(r_m)]^{M_1}/[G(r_m)]^{M_2} = G^{M_1 M_2}(r_m). \quad (22)$$

We have $G(r_m) < 1$, so arrangements with small M will be the most probable, since the number M at a distance of several ion diameters may reach a few dozen. The competition between different spatial orientations of the triplets
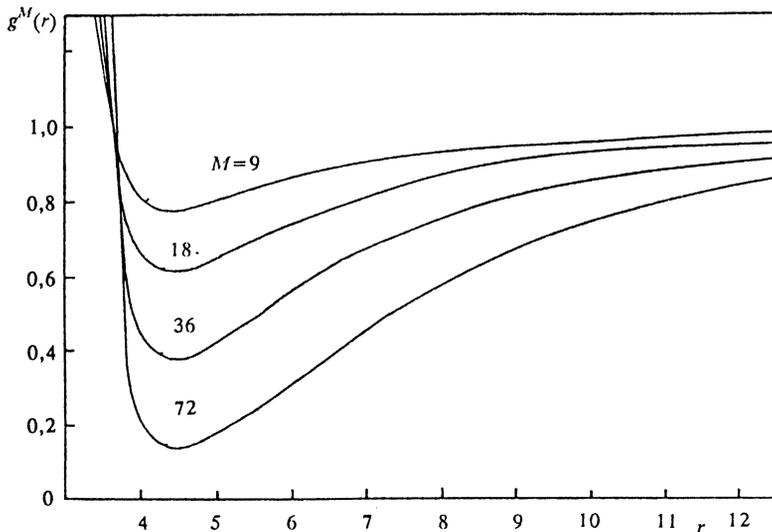

FIG. 11. Collective cluster distribution in model 2 for $T=0.1$: the probability density for observing M triplets simultaneously at a distance r from a specified triplet, disregarding triple correlations among them, normalized with respect to the volume.

in the microdroplet can be quite close even when the minimum in $G(r)$ is relatively shallow (Fig. 11), which determines the density profile of the latter.

If the microdroplet has spherical symmetry, the minimum value of M corresponds to arrangements of triplets on the surface. A hollow with a reduced density develops inside the small system, and the overall volume of the small system increases due to the repulsion of the particles toward the surface. If the size of the microdroplet is comparable with r_m, almost all particles of the microdroplet are at energetically unfavorable distances from the ion triplet in the interior region, $M \sim N$. When an ion triplet shifts toward the surface the value of M corresponding to it decreases severalfold.

The repulsion of the ion triplets in the 2–1-valent microsystem can be interpreted as an additional internal pressure balancing the external pressure of the macrosystem. Consequently the formation of microdroplets of size r_m will be inhibited, i.e., will occur at higher pressures and lower temperatures. On the other hand, as the temperature decreases the value of r_m increases, and along with it so do the energetically unfavorable distances. If the energetically unfavorable interactions are found outside the characteristic dimensions of the microdroplet, condensation into a microdroplet becomes thermodynamically favored. According to our preliminary estimates, the effect of slowing down of microcondensation due to the repulsion of ion triplets must be exhibited most clearly for microdroplets of 10^2–10^3 ions.

The competition between two factors, attraction at short distances and repulsion at intermediate ones, determines the thermodynamic stability of the dense phase. In a small system the ions are distributed so as to minimize the number of pairwise interactions between triplets at distances close to r_m, while at the same time maintaining the interactions at short distances. A compromise solution is found by distributing the density of the small system nonuniformly while maintaining spherical symmetry.

The selection of attractive orientations of the fourth kind from the whole set of orientations as the temperature decreases implies that orientational order develops at short distances. Thus, the necessary condition for the formation of a stable dense phase from a gas of ion triplets is orientational close ordering. In a macroscopic uniform system there are no surface particles, and the average number of nearest neighbors is larger than in a small system with the same conditions otherwise. Consequently, orientational close ordering must develop here at higher temperatures than in a small system.

[1]Here and in what follows all numerical data are given in the natural system of units: the unit of distance is taken to be the ion diameter, the unit of charge is taken to be the charge of the negative ion, and the Boltzmann constant is set equal to unity.

[1] J. E. Mayer, J. Chem. Phys. 5, No. 1, 67 (1937).
[2] J. E. Mayer and P. G. Ackermann, J. Chem. Phys. 5, No. 1, 74 (1937).
[3] J. E. Mayer, J. Chem. Phys. 18, No. 11, 1426 (1950).
[4] J. E. Mayer, J. Chem. Phys. 19, No. 8, 1024 (1951).
[5] E. Haga, J. Phys. Soc. Jpn. 8, No. 6, 714 (1953).
[6] J. C. Poirier, J. Chem. Phys. 21, No. 6, 965, 972 (1953).

[7] E. Salpeter, Ann. Phys. 5, No. 4, 183 (1958).
[8] E. Meeron, J. Chem. Phys. 28, No. 4, 630 (1958).
[9] H. L. Friedman, Mol. Phys. 2, No. 1, 23 (1959).
[10] H. L. Friedman, Mol. Phys. 2, No. 2, 190 (1959).
[11] R. Abe, Progr. Theor. Phys. 22, No. 2, 213 (1959).
[12] H. Ll. Friedman, Ionic Solution Theory, New York-London (1962).
[13] H. L. Frisch, Adv. Chem. Phys. 6, 229 (1964).
[14] G. Stell and J. L. Lebowitz, J. Chem. Phys. 49, No. 8, 3706 (1968).
[15] D. Henderson and L. Blum, Mol. Phys. 40, No. 6, 1509 (1980).
[16] A. Ichihara, Statistical Physics, Academic, New York (1971).
[17] R. Balescu, Statistical Mechanics of Charged Particles, Interscience, New York (1963).
[18] Yu. L. Klimontovich, Statistical Physics, Harwood, New York (1986).
[19] V. A. Fock, The Principles of Quantum Mechanics [Russian translation], Mir, Moscow (1978).
[20] L. D. Landau and E. M. Lifshitz, Quantum Mechanics, 3rd ed., Pergamon, Oxford (1977).
[21] A. S. Davydov, Quantum Mechanics, 2nd ed., Pergamon, Oxford (1976).
[22] N. Metropolis, A. W. Rosenbluth, M. N. Rosenbluth, and E. A. Teller, J. Chem. Phys. 21, No. 6, 1087 (1953).
[23] M. N. Rosenbluth and A. W. Rosenbluth, J. Chem. Phys. 22, No. 5, 881 (1954).
[24] B. J. Alder, S. P. Frankel, and V. A. Lewinson, J. Chem. Phys. 23, No. 3, 417 (1955).
[25] W. W. Wood and J. D. Jacobson, J. Chem. Phys. 27, No. 5, 1207 (1957).
[26] B. J. Alder and T. E. Wainwright, J. Chem. Phys. 27, No. 5, 1208 (1957).
[27] B. J. Alder and T. E. Wainwright, J. Chem. Phys. 31, No. 2, 459 (1959).
[28] B. J. Alder and T. E. Wainwright, J. Chem. Phys. 33, No. 5, 1439 (1960).
[29] B. J. Alder and T. E. Wainwright, Phys. Rev. 127, No. 2, 359 (1962).
[30] W. G. Hoover and B. J. Alder, J. Chem. Phys. 46, No. 2, 686 (1968).
[31] B. J. Alder, W. G. Hoover, and D. A. Young, J. Chem. Phys. 49, No. 8, 3688 (1968).
[32] A. Rotenberg, J. Chem. Phys. 42, No. 3, 1126 (1965).
[33] W. G. Hoover and H. F. Ree, J. Chem. Phys. 49, No. 8, 3609 (1968).
[34] W. W. Wood, J. Chem. Phys. 48, No. 1, 415 (1968).
[35] E. J. LeFebre, Nature, 235, No. 53, p. 20 (1972).
[36] D. J. Adams, Mol. Phys. 28, No. 5, 1241 (1974).
[37] K. W. Johnson, D. Henderson, J. A. Barker, and B. C. Brown, J. Chem. Phys. 52, No. 10, 4931 (1970).
[38] W. G. Hoover, S. G. Gray, and K. W. Johnson, J. Chem. Phys. 55, No. 3, 1128 (1971).
[39] L. D. Landau and E. M. Lifshitz, Statistical Physics, Part I, Pergamon, Oxford (1980).
[40] T. L. Hill, Thermodynamics of Small Systems, Vols. 1 and 2, New York-Amsterdam (1963).
[41] T. L. Hill, Statistical Mechanics. Principles and Selected Applications, McGraw-Hill, New York (1956).
[42] A. C. Zettlemoyer (ed.), Nucleation, Dekker, New York (1969).
[43] J. Frenkel, J. Chem. Phys. 7, No. 3, 200 (1939).
[44] W. Band, J. Chem. Phys. 7, No. 5, 324 (1939).
[45] W. Band, J. Chem. Phys. 7, No. 10, 927 (1939).
[46] J. Frenkel, J. Chem. Phys. 7, No. 7, 538 (1939).
[47] P. Debye and E. Hückel, Phys. Z. 24, No. 9, 185 (1923).
[48] J. G. Kirkwood and J. C. Poirier, J. Phys. Chem. 58, No. 7, 591 (1954).
[49] G. A. Martynov, Usp. Fiz. Nauk 91, No. 3, 455 (1967).
[50] J. D. Ramshaw, J. Chem. Phys. 64, No. 9, 3666 (1976).
[51] J. D. Ramshaw, J. Chem. Phys. 73, No. 8, 3695 (1980).
[52] D. D. Carley, J. Chem. Phys. 46, No. 10, 3783 (1967).
[53] J. C. Rasaiah and H. L. Friedman, J. Chem. Phys. 48, No. 6, 2742 (1968).
[54] J. C. Rasaiah and H. L. Friedman, J. Chem. Phys. 50, No. 9, 3965 (1969).
[55] E. Waisman and J. L. Lebowitz, J. Chem. Phys. 52, No. 8, 4307 (1970).
[56] G. A. Martynov, Teor. Mat. Fiz. 22, No. 2, 260 (1975).
[57] M. Baus and J. P. Hansen, J. Phys. C12, No. 2, L55 (1979).
[58] G. A. Martynov and A. B. Shmidt, Teplofiz. Vys. Temp. 17, No. 2, 278 (1979).
[59] J. Wiechen, J. Chem. Phys. 85, No. 12, 7364 (1986).

[60] G. Pastore, P. V. Giaquinta, J. S. Thakur, and M. P. Rosi, J. Chem. Phys. **84**, No. 3, 1827 (1986).

[61] P. N. Vorontsov-Vel'yaminov, A. M. El'yashevich, and A. K. Kron, Élektrokhim. **2**, No. 6, 708 (1966).

[62] P. N. Vorontsov-Vel'yaminov and A. M. El'yashevich, Élektrokhim. **4**, No. 12, 1430 (1968).

[63] D. N. Card and J. P. Valleau, J. Chem. Phys. **52**, No. 12, 6232 (1970).

[64] P. N. Vorontsov-Veliaminov, A. M. Eliashevich, J. C. Rasaiah, and H. L. Friedman, J. Chem. Phys. **52**, No. 2, 1013 (1970).

[65] J. C. Rasaiah, D. N. Card, and J. P. Valleau, J. Chem. Phys. **56**, No. 6, 248 (1972).

[66] A. Rahman, R. H. Fowler, and A. H. Narten, J. Chem. Phys. **57**, No. 7, 3010 (1972).

[67] D. J. Adams and I. R. McDonald, J. Phys. **C7**, No. 16, 2761 (1974).

[68] Ch. Margheritis and C. Sinistri, Z. Naturforsch. **30a**, No. 1, 83 (1975).

[69] G. Ciccotti and J. Jacucci, Phys. Rev. **13A**, No. 1, 426 (1976).

[70] J. W. E. Lewis, K. Singer, and L. V. Woodcock, J. Chem. Soc. Faraday Trans. 2 **71**, No. 2, 301 (1975).

[71] J. W. E. Lewis and K. Singer, J. Chem. Soc. Faraday Trans. **71**, No. 1, 41 (1975).

[72] L. V. Woodcock, Chem. Phys. Lett. **10**, No. 3, 257 (1971).

[73] J. P. Valleau and D. N. Card, J. Chem. Phys. **57**, No. 12, 5457 (1972).

[74] V. P. Chasovskikh and P. N. Vorontsov-Vel'yaminov, Teplofiz. Vys. Temp. **14**, No. 2, 379 (1976).

[75] P. N. Vorontsov-Vel'yaminov and V. P. Chasovskikh, *Bulletin of Leningrad State University*, No. 2, Issue 2, 30 (1975).

[76] B. V. Zelener, G. É. Norman, and V. S. Filinov, Teplofiz. Vys. Temp. **22**, No. 5, 922 (1973).,

[77] P. N. Vorontsov-Vel'yaminov and V. K. Shiff, Teplofiz. Vys. Temp. **15**, No. 6, 1137 (1977).

[78] B. Larsen, T. Forland, and K. Singer, Mol. Phys. **26**, No. 6, 1521 (1973).

[79] V. P. Chasovskikh and P. N. Vorontsov-Vel'yaminov, Teplofiz. Vys. Temp. **14**, No. 1, 199 (1974).

[80] P. N. Vorontsov-Vel'yaminov, A. M. El'yashevich, L. A. Morgenshtern, and V. P. Chasovskikh, Teplofiz. Vys. Temp. **8**, No. 2, 277 (1970).

[81] V. P. Chasovskikh, P. N. Vorontsov-Vel'yaminov, A. M. El'yashevich, and A. N. Nurullaev, Dokl. Akad. Nauk Tadzh. SSR **16**, No. 2, 26 (1973).

[82] V. P. Chasovskikh, P. N. Vorontsov-Vel'yaminov, and A. M. El'yashevich, Dokl. Akad. Nauk Tadzh. SSR **16**, No. 5, 30 (1973).

[83] V. P. Chasovskikh, P. N. Vorontsov-Vel'yaminov, and A. M. El'yashevich, Dokl. Akad. Nauk Tadzh. SSR **16**, No. 10, 23 (1973).

[84] P. N. Vorontsov-Vel'yaminov and V. P. Chasovskikh, Teplofiz. Vys. Temp. **14**, No. 6, 1153 (1975).

[85] B. Larsen, Chem. Phys. Lett. **27**, No. 1, 47 (1974).

[86] P. N. Vorontsov-Vel'yaminov and V. K. Shiff, Deposited Paper No. 3783-78, VINITI, December 12, 1978.

[87] P. N. Vorontsov-Vel'yaminov and V. K. Shiff, Deposited Paper No. 2086-79, VINITI, September 3, 1979.

[88] A. D. Kurschenbaum, J. A. Cahill, P. J. McGonigal, and A. V. Grosse, J. Inorg. Nucl. Chem. **24**, 1287 (1962).

[89] S. V. Shevkunov and P. N. Vorontsov-Vel'yaminov, Teplofiz. Vys. Temp. **21**, No. 4, 625 (1983).

[90] S. V. Shevkunov, P. N. Vorontsov-Vel'yaminov, and H. B. Gromova, Teplofiz. Vys. Temp. **24**, No. 5, 998 (1986).

[91] V. K. Shiff, Deposited Paper No. 3074-80, VINITI, July 15, 1980.

[92] V. K. Shiff, Teplofiz. Vys. Temp. **24**, No. 5, 1020 (1986).

[93] V. K. Shiff, Teplofiz. Vys. Temp. **26**, No. 6, 1072 (1988).

[94] P. N. Vorontsov-Vel'yaminov and S. V. Shevkunov, Fiz. Plazmy **4**, No. 6, 1354 (1978) [Sov. J. Plasma Phys. **4**, 756 (1978)].

[95] S. V. Shevkunov and P. N. Vorontsov-Vel'yaminov, Teplofiz. Vys. Temp. **20**, No. 6, 1025 (1982).

[96] S. V. Shevkunov and P. N. Vorontsov-Vel'yaminov, Khim. Fiz. No. 1, 83 (1983).

[97] T. P. Martin, J. Chem. Phys. **72**, No. 6, 3506 (1980).

[98] A. A. Marsinovski, S. V. Shevkunov, and P. N. Vorontsov-Vel'yaminov, Mol. Sim. **6**, No. 1, 2, 46 (1990).

[99] P. N. Vorontsov-Vel'yaminov and V. A. Pavlov, Teplofiz. Vys. Temp. **13**, No. 2, 302 (1975).

Translated by David L. Book